Centaurus A as the source of ultrahigh-energy cosmic rays?

Claudia Isola, Martin Lemoine, Günter Sigl

Centaurus A as the source of ultrahigh-energy cosmic rays?

Claudia Isola
Centre de Physique Théorique, Ecole Polytechnique, 91128 Palaiseau Cedex, France

Martin Lemoine and Günter Sigl
Institut d'Astrophysique de Paris, C.N.R.S., 98 bis boulevard Arago, F-75014 Paris, France

(Received 17 April 2001; published 26 December 2001)

We present numerical simulations for energy spectra and angular distributions of nucleons above 10^{19} eV injected by the radio-galaxy Centaurus A at a distance 3.4 Mpc and propagating in extra-galactic magnetic fields in the submicro Gauss range. We show that field strengths $B \simeq 0.3\ \mu$G, as proposed by Farrar and Piran, cannot provide sufficient angular deflection to explain the observational data. A magnetic field of intensity $B \simeq 1\ \mu$G could reproduce the observed large-scale isotropy and could marginally explain the observed energy spectrum. However, it would not readily account for the $E = 320 \pm 93$ EeV Fly's Eye event that was detected at an angle 136° away from Cen-A, and it saturates observational upper bounds on the strength of extra-galactic magnetic fields. High energy cosmic ray experiments now under construction will be able to detect the level of anisotropy predicted by this scenario. We conclude that for magnetic fields $B \simeq 0.1$–$0.5\ \mu$G, considered as more reasonable for the local supercluster environment, in all likelihood at least a few sources within $\simeq 10$ Mpc from the Earth should contribute to the observed ultrahigh-energy cosmic ray flux.

DOI: 10.1103/PhysRevD.65.023004 PACS number(s): 98.70.Sa, 13.85.Tp, 98.54.Cm

I. INTRODUCTION

In acceleration scenarios ultrahigh-energy cosmic rays (UHECRs) with energies above 10^{18} eV are assumed to be protons accelerated in powerful astrophysical sources. During their propagation, for energies above $\gtrsim 50$ EeV (1 EeV $= 10^{18}$ eV) they lose energy by pion production and pair production (protons only) on the microwave background. For sources further away than a few dozen Mpc this would predict a break in the cosmic ray flux known as the Greisen-Zatsepin-Kuzmin (GZK) cutoff [1], around 50 EeV. This break has not been observed by experiments such as Fly's Eye [2], Haverah Park [3], Yakutsk [4], Hires [5] and AGASA [6], which instead show an extension beyond the expected GZK cutoff and events above 100 EeV. This situation has in recent years triggered many theoretical explanations ranging from conventional acceleration in astrophysical sources to models invoking new physics such as the top-down scenarios in which energetic particles are produced in the decay of massive relics from the early Universe. This enigma has also fostered the development of large new detectors of ultrahigh-energy cosmic rays which will increase very significantly the statistics at the highest energies [7].

In bottom-up scenarios of UHECR origin, in which protons are accelerated in powerful astrophysical objects such as hot spots of radio galaxies and active galactic nuclei [8], one would expect to see the source in the direction of arrival of UHECRs. The lack of observed counterparts to the highest energy events [9,10] implies the existence of large scale intervening magnetic fields with intensity $B \sim 0.1$–$1\ \mu$G [10], which would provide sufficient angular deflection, or bursting sources and a magnetic field of intensity $B \gtrsim 10^{-11}$ G which would impart sufficient time delay to UHE protons to explain their lack of correlation in time of arrival with optical or high energy photons [11]. It has been realized recently that magnetic fields as strong as $\simeq 1\ \mu$G in sheets and filaments of large scale structure, such as our local supercluster, are compatible with existing upper limits on Faraday rotation [12–14]. The origin of such magnetic fields is yet another enigma, but there is evidence for the existence of ordered magnetic fields with strength $\sim \mathcal{O}(0.1\ \mu\text{G})$ on supracluster scales [15].

Such strong magnetic fields would have profound consequences for the propagation of charged ultrahigh-energy cosmic rays [16–18]. In particular in the presence of a magnetic field of strength $B \simeq 0.1\ \mu$G, and for a source at distance $\simeq 10$ Mpc, UHECR protons with energy $E \lesssim 100$ EeV would diffuse, while higher energy cosmic rays would propagate rectilinearly. The resulting modification of the energy spectrum would explain naturally the observed spectrum for a unique power-law injection of index $\simeq 2.2$. In Ref. [18], we further showed that a large number of such sources in the local supercluster, at distance scale $\simeq 10$ Mpc with an ambient magnetic field $B \simeq 0.1\ \mu$G would explain the large scale isotropy of arrival directions observed by the Akemo Giant Air Shower Array (AGASA) [6]. It could also explain the observed small-scale angular clustering (five doublets and one triplet within 2.5° out of 57 events above 40 EeV) by magnetic lensing effects through the large scale turbulent magnetic field.

At first sight this suggests the possibility of having only one object in the Sky as the source of all UHECRs with $E \gtrsim 5$ EeV, including the highest energy events. Two versions of such single source scenarios have recently been put forward in the literature: one with an extreme version of a coherent galactic magnetic wind structure in which all observed UHECRs supposedly can be traced back to M87 in the Virgo cluster [19], and a second one with Centaurus A at 3.4 Mpc distance with an all-pervading magnetic field of intensity $B \simeq 0.3\ \mu$G [20]. In the present paper we examine critically the latter of these scenarios using detailed numerical simulations for the energy spectrum and the angular dis-

tribution of ultrahigh-energy nucleons propagating in magnetic fields of rms strength between 0.3 and 1 μG. Since we want to test specifically the scenario proposed in Ref. [20], we consider only UHECR nucleons and not heavy nuclei, and it is understood that all that follows applies to nucleon primaries only. In Sec. IV we briefly discuss how our conclusions would be changed if heavy nuclei were the primaries, and indeed it appears to be an interesting loophole in our argument against Cen-A as the source of all UHECRs.

Typical proton deflection angles in galactic magnetic fields of several μG are $\lesssim 10°$ above 4×10^{19} eV [21,22] and thus small compared to deflection in $\gtrsim 0.3$ μG fields extended over megaparsec scales, and therefore we will neglect the galactic contribution to the deflection of UHECR nucleons. An exception is given by the scenario mentioned above which invokes a particular wind like configuration of the galactic magnetic field extended over ~ 1 Mpc [19].

II. NUMERICAL SIMULATIONS

Trajectories are calculated from the Lorentz equation in a given magnetic field and pion production is treated as stochastic energy loss while pair production is included into the equations of motion as a continuous energy loss term. This numerical tool has been used and discussed in earlier publications [17,18].

We assume a homogeneous random turbulent magnetic field with power spectrum $\langle B(k)^2\rangle \propto k^{n_B}$ for $2\pi/L < k < 2\pi/l_c$ and $\langle B^2(k)\rangle = 0$ otherwise. We use $n_B = -11/3$, corresponding to Kolmogorov turbulence, in which case L, the largest eddy size, characterizes the coherence length of the magnetic field; we use $L \simeq 1$ Mpc, which corresponds to about one turn-around in a Hubble time. Physically one expects $l_c \ll L$, but numerical resolution limits us to $l_c \gtrsim 0.008L$. We generally use $l_c \simeq 0.03$ Mpc, but we checked by increasing the resolution for several runs that it has no effect on the results discussed in the following. The magnetic field modes are dialed on a grid in momentum space according to this spectrum with random phases and then Fourier transformed onto the corresponding grid in location space. The rms strength B is given by $B^2 = \int_0^\infty dk\, k^2 \langle B^2(k)\rangle$.

Typically, 5000 trajectories are computed for each magnetic field realization obtained in this way for 10–20 realizations in total. Each trajectory is followed for a maximal time of 10 Gyr and as long as the distance from the observer is smaller than double the source distance. We have also checked that the results do not significantly depend on these cut-offs. Furthermore, the distance limit is reasonable physically as it mimics a magnetic field concentrated in the large scale structure, with much smaller values in the voids, as generally expected.

In Fig. 1, we show the angular distribution of UHE events as seen on Earth in equatorial coordinates, for two ranges of energies $E \gtrsim 40$ EeV, and $E \gtrsim 100$ EeV, and for $B = 0.3$ μG, with Cen-A as the source. These images are averaged over different spatial realizations of the magnetic field. The distributions for specific realisations are more anisotropic than the average due to cosmic variance. The angular distribution predicted by this one source model is thus not

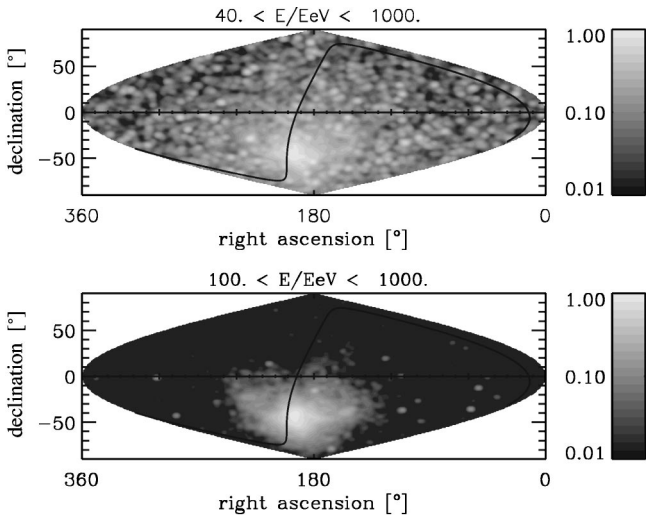

FIG. 1. The angular image in terrestrial coordinates, averaged over all 20 magnetic field realizations of 5000 trajectories each, for events above 40 EeV (upper panel) and above 100 EeV (lower panel), as seen by a detector covering all Earth, for the case suggested in Ref. [20] corresponding to $B = 0.3$ μG, and the source Cen-A located 3.4 Mpc away. The grey scale represents the integral flux per solid angle. The solid line marks the supergalactic plane. The pixel size is 1°; the image has been convolved to an angular resolution of 2.4° corresponding to AGASA.

consistent with the isotropic distribution deduced by experimental data [2,6]. This is even more clearly demonstrated by Fig. 2, which gives the distribution in declination of arrival coordinates of UHE events. The source Cen-A is located at RA = 201.3°, $\delta = -43.0°$ in equatorial coordinates, and corresponds to the peak of flux in Figs. 1,2.

Cen-A does not lie in the field of view of experiments that have provided data so far such as the Fly's Eye and AGASA. This and the fact that the angular deflection of particles with

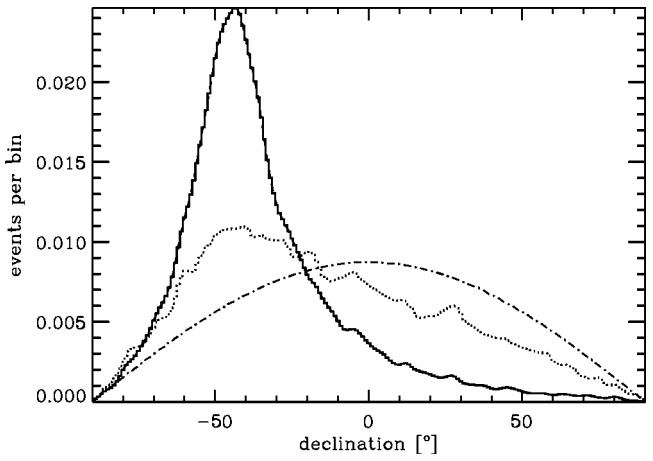

FIG. 2. The distribution of arrival declination on Earth, averaged over many realizations, for $E \geqslant 40$ EeV (dotted line) and $E \geqslant 100$ EeV (solid line), for the scenario corresponding to Figs. 1. The dash-dotted line represents an isotropic distribution. The pixel size is 1° and the image has again been convolved with an angular resolution of 2.4°.

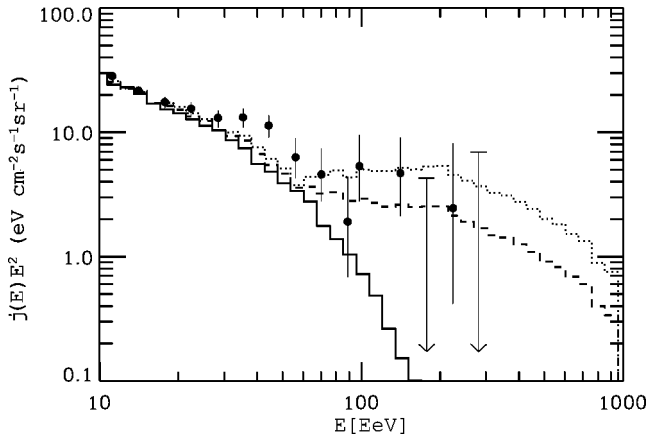

FIG. 3. The realization averaged energy spectra corresponding to Figs. 1,2. The solid line represents the spectrum that would have been detected by AGASA, and has been obtained from Eq. (1). The dashed line indicates the spectrum uniformly averaged over the whole sky. The dotted line is the spectrum predicted by an AGASA type experiment in the Southern hemisphere. The one sigma error bars indicate the AGASA data. The various spectra have been normalized to optimally fit the AGASA flux. Significant uncertainties due to cosmic variance and parameters such as the largest eddy size L only occur for energies between $\simeq 70$ EeV and a few hundred EeV where they are still smaller than a factor $\simeq 2.5$.

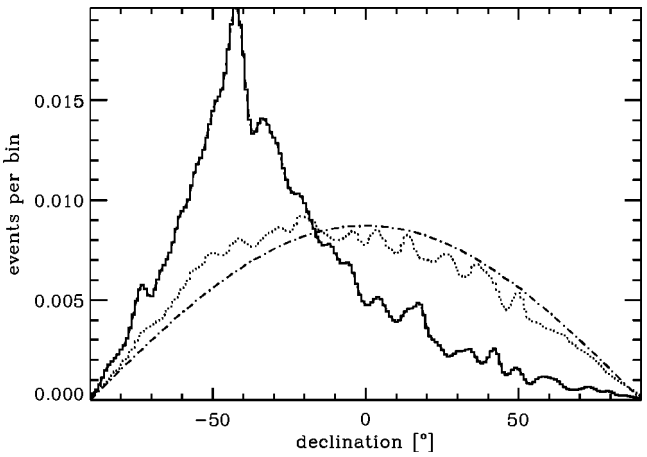

FIG. 4. The distribution of arrival declination on Earth, averaged over many realizations, for $E \geqslant 100$ EeV (dotted line) and $E \geqslant 300$ EeV (solid line). All other parameters are as in Fig. 2, expect $B=1$ μG.

$E \gtrsim 100$ EeV is relatively small has an important consequence for the energy spectrum predicted by this model: The Northern hemisphere experiments should never have detected the highest energy events, for which the angular deflection is too weak to bring the particle in the field of view. This is made clear in Fig. 3, where we compare the spectrum predicted for AGASA with the actually observed spectrum, assuming an injection spectrum $\propto E^{-2}$ up to 10^{21} eV. The prediction is obtained by folding the simulated distribution in energy E and arrival direction Ω, $D(E,\Omega)$, with the normalized AGASA exposure function AGASA(δ) (which to a good approximation only depends on declination δ):

$$j(E) \equiv \int \mathrm{d}\,\Omega D(E,\delta)\mathrm{AGASA}(\delta). \qquad (1)$$

For reference, we also show in Fig. 3 the spectrum that would be observed by an idealized detector covering the whole sky uniformly, and by a mirror AGASA experiment located in the Southern hemisphere. The solid angle integrated spectrum $\int \mathrm{d}\Omega D(E,\delta)$ observed by a uniform detector is still different from the injection spectrum ($\propto E^{-2}$) at low energies, while the two match at high energies. This results from an increased local residence time due to diffusion at low energies, and rectilinear propagation (hence unaffected energy spectrum) at high energies [17]. The pile-up around $E \simeq 40$ EeV due to pion production of higher energy particles, also contributes to the change of slope at low energies.

The scenario just discussed, which is already ruled out by the energy spectrum and large-scale isotropy recorded by Northern hemisphere detectors, has been proposed by Farrar and Piran [20] on analytical grounds to explain all observational data. The discrepancy, as will be discussed in greater detail in Sec. III, results from the fact that they argued that diffusion held up to the highest energies, whereas in fact the diffusion approximation breaks for $E \gtrsim 100$ EeV, implying much larger anisotropies at these energies. The impact of angular anisotropy on the energy spectrum for a source located in the blind area of northern hemisphere detectors had also been overlooked in Ref. [20].

For the scenario with $B=0.3$ μG we have also established a rough estimate of the minimal number of sources necessary to explain existing observations in the following way: we overlayed distributions from single sources in random directions (for simplicity chosen to be at equal distances as Cen-A) and computed the average and fluctuations of the declination distributions of UHECR arrival directions. The minimal number of sources is determined by requiring that the distribution is consistent with isotropy within the fluctuations and turns out to be 5–10. This number is a crude estimate and one should allow for different distances for the different sources, and study the dependence of this number on the magnetic field properties; such analysis is clearly beyond the scope of the present paper, but will be performed in a subsequent study.

We now investigate whether stronger magnetic fields, by providing larger angular deflection, might provide a better match to the observational data. In particular, we focus on the case where $B=1$ μG, and Cen-A is again the unique source of UHECRs. One should stress that there is no observational evidence for such strong extragalactic magnetic fields [23], although one cannot rule it out either on observational grounds (see below). As we show below, the single source model is therefore rather contrived as it requires a very strong magnetic field, but this latter remains a possibility, and cannot be discarded altogether.

The resulting arrival distribution in declination is shown for several ranges of energies in Fig. 4, and the resulting energy spectra, calculated as before, are shown in Fig. 5. Increasing the magnetic field strength increases the maximal energy at which diffusion takes place, hence it decreases the anisotropy at each energy up to that maximal energy, and

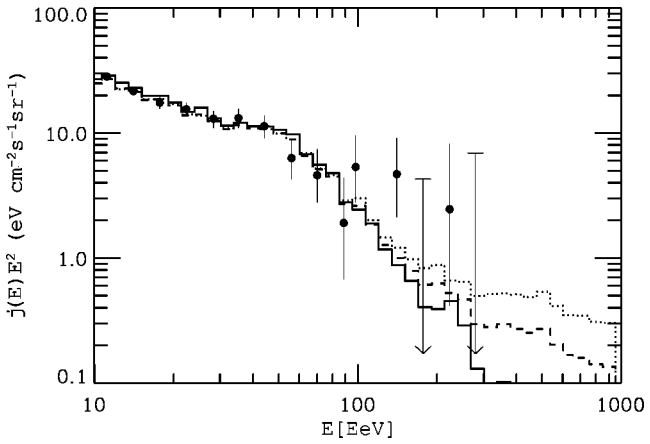

FIG. 5. Normalization averaged energy spectra with the same conventions as in Fig. 3, but for $B=1\ \mu$G, all other parameters being equal.

thus reduces the differences between the spectra seen by different detectors (AGASA, uniform, and Southern hemisphere analogue of AGASA).

The large-scale anisotropy in this case is much smaller and could not have been detected by northern hemisphere experiments such as the Fly's Eye and AGASA. The predicted energy spectrum for AGASA does not provide a very good fit to the observed spectrum, see Fig. 5, but the difference is not sufficient to rule out this scenario on this ground. However, we note that it is unlikely that the highest energy Fly's Eye event would have been detected in this model. This event of energy $E=320\pm93$ EeV makes an angle of 136° with the line of sight to Cen-A [10]. By folding the energy probability distribution for the Fly's Eye event with the simulated distribution of deflection angles and energies one finds that 95% of events with a recorded energy corresponding to the Fly's Eye event are deflected less than $\simeq 130°$.

Thus the present observational evidence is not sufficient to rule out with a high degree of confidence the possibility that Cen-A is the source of all ultrahigh-energy cosmic rays, *if* the intervening magnetic field $B\gtrsim 1\ \mu$G. Notably, one cannot rule out the possibility of having a magnetic configuration different from Kolmogorov turbulence, in which case the modification of the energy spectrum would be different than what is shown in the present simulations. For instance, it has been proposed that the magnetic field is not all pervading, but strongly enhanced in regions close to radio-galaxies that were active in the past [10,24], in which case the configuration seen by UHECRs would be a collection of scattering centers rather than Kolmogorov turbulence.

However, if future or ongoing experiments in the Northern hemisphere, e.g. the High Resolution Fly's Eye [5] and AGASA [6] keep recording cosmic rays above $\simeq 200$ EeV with large deflection angles from the line of sight to Cen-A, even the scenario with $B\simeq 1\ \mu$G would be ruled out. Similarly, if no significant anisotropy is seen between these experiments and the southern Pierre Auger array [25] at the highest energies, the model would be discarded. As an example, we calculate from Eq. (1) the fractional difference $\delta I\equiv(I_{\rm N}-I_{\rm S})/(I_{\rm N}+I_{\rm S})$ of integral fluxes $I_{\rm N}$ and $I_{\rm S}$ that would be seen by detectors in the Northern and Southern hemispheres above a given energy (for simplicity, we use exposure functions for AGASA and an analogous one for the Southern hemisphere, as before). We find $\delta I\simeq -0.19$ for $E\gtrsim 100$ EeV, and $\delta I\simeq -0.78$ for $E\gtrsim 300$ EeV. These numbers can also very roughly been estimated from Fig. 4. There are several planned full sky observatories which will easily be able to detect anisotropies of this size. The Pierre Auger project [25] will consist of one hybrid array of water tanks and fluorescence detectors in each hemisphere of which the southern one is currently under construction in Argentina. For a total acceptance of 7000 km^{2}sr [26] per array and the flux predictions shown in Fig. 5 one would need $\simeq 6$ and $\simeq 2$ years to detect the anisotropy δI at the 3σ level above 100 EeV and above 300 EeV, respectively. This would correspond to detect $\simeq 220$ and $\simeq 8$ events in total (i.e. the northern and southern array combined), respectively. There are furthermore plans for space based air shower detectors such as OWL [27] and EUSO [28]. Although the design of these projects is not worked out yet in detail, they are likely to have even higher acceptances than the Pierre Auger Observatories.

We note in this context that we have assumed in all our simulations that the source emits only protons. If the source is sufficiently compact, protons could convert into neutrons within the source. As pointed out in Ref. [29], for sources as close as Cen-A, neutrons at the highest energies could survive decay and produce a spike in the direction of the source. This can only increase anisotropy. Preliminary simulations performed with our code indicate that the total flux in the $\simeq 2°$ pixel centered on the source is significantly (i.e. by a factor $\simeq 2$) increased only above $\simeq 300$ EeV.

We stress that $B\simeq 1\ \mu$G corresponds to the upper limit inferred on the strength of the magnetic field in the local supercluster from Faraday rotation observations of distant quasars [12–14]. Strictly speaking, the rotation measure is a function of $B\sqrt{L}$, where L denotes as before the coherence scale of the field, provided that $L\ll R$, where R represents the size of the medium pervaded by the magnetic field (for the local supercluster $R\simeq 10-50$ Mpc). In principle, the coherence length L could be smaller than 1 Mpc, used in the previous section, and B correspondingly larger. However, as will be discussed in the next section, the diffusion coefficient $D(E)$ scales inversely proportional with L, so that by decreasing L, one would increase $D(E)$ correspondingly, and the diffusion approximation would break down at a smaller energy, thereby increasing the anisotropy at higher energies. We thus find that one cannot decrease L and increase B to improve the fit to the data. Moreover, notwithstanding this fact, if diffusion were to be more efficient at the highest energies observed, the effective distance traveled would be consequently increased, and the GZK cutoff would be more pronounced, which would further aggravate the disagreement with the observed spectrum.

We thus conclude that $B\simeq 1\ \mu$G seems to be the only value of B that would be marginally consistent with Cen-A as the source of observed UHECRs. We further note that if equipartition of energy holds, the magnetic field intensity is tied to the thermal energy density of the ambient gas:

$$B = 0.5 \ \mu\mathrm{G}\, T_7^{1/2} \kappa_{10}^{1/2} h_{70}, \tag{2}$$

where $T_7 \equiv T/10^7$ K is the temperature of the local supercluster in units of 10^7 K, and $\kappa_{10} \equiv \kappa/10$, with κ the collapse factor (i.e., the local overdensity of baryons and electrons), and h_{70} the Hubble constant in units of 70 km/s/Mpc. The gas cools by bremsstrahlung emission in the keV range, which in principle can be observed. A marginal detection of x-ray emission correlated with the plane of the local supercluster has actually been reported and corresponds to a collapse factor $\kappa_{10} \simeq 1$, with a weak dependence on the assumed temperature $T \simeq 10^8$ K [30]; the signal is however weak and these parameters could be in error. Numerical simulations of large-scale structure formation indicate that $\kappa_{10} \simeq 1$ and $T \simeq 10^7$ K are probably upper limits for sheets such as the local supercluster, and seem to better describe the filamentary structures [13]. Deep searches for soft x-ray emission correlated with the plane of the local supercluster using the XMM-Newton or Chandra observatories could improve these limits, and appear mandatory.

Finally one should point out that the arrival direction distributions predicted for $B \gtrsim 0.3$ μG tend to produce spikes with small angular width which could correspond to the event clusters seen by various experiments, notably AGASA [6]. This effect is due to caustics effects in magnetic lensing as shown numerically in a previous work [18], and studied analytically in Ref. [31]. However, since clustering would need more extensive numerical simulations to be properly quantified through the calculation of the angular two-point correlation function [36], and since the large scale angular distributions already suffices to rule out the single source model for $B \lesssim 1$ μG, we do not pursue this analysis in the present case.

III. COMPARISON WITH ANALYTICAL ESTIMATES

Let us now compare these results with analytical estimates in an approach similar to [20]. There is often confusion in the literature about different regimes of diffusion and corresponding expressions for the diffusion coefficient. It is dangerous to take analytical expressions too literally as there exists no analytical derivation of diffusion coefficients in the limit in which the turbulent component of the magnetic fields becomes comparable or stronger than a (putative) uniform component, the so-called strong turbulence regime. In this respect, one should note that the formula for the diffusion coefficient given in Ref. [16], now used without caution in the community, does not correspond to an analytical derivation. It is a phenomenological formula, that is furthermore shown to be in error in Ref. [32], where analytical approximations and accurate measurements of diffusion coefficients obtained through Monte Carlo simulations are presented. Notably, this latter study shows that for Kolmogorov turbulence the diffusion coefficient can be approximated as

$$\begin{aligned} D(E) &\simeq 0.02 E_{20}^{7/3} B_{-6}^{-7/3} L_{\mathrm{Mpc}}^{-4/3} \ \mathrm{Mpc}^2/\mathrm{Myr}, \quad E_c < E_{20}, \\ &\simeq 0.03 E_{20} B_{-6}^{-1} \quad \mathrm{Mpc}^2/\mathrm{Myr}, \quad 0.1 E_c < E_{20} < E_c, \\ &\simeq 0.004 E_{20}^{1/3} B_{-6}^{-1/3} L_{\mathrm{Mpc}}^{-2/3} \ \mathrm{Mpc}^2/\mathrm{Myr}, \quad E_{20} < 0.1 E_c. \end{aligned} \tag{3}$$

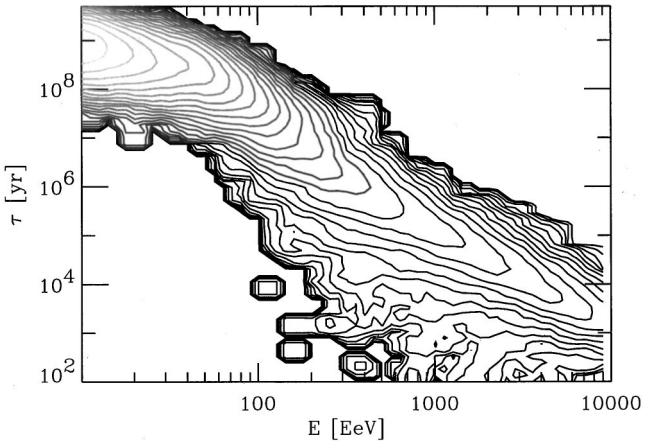

FIG. 6. Distribution of time delays τ versus recorded energy E, for $B = 1$ μG, and Cen-A as the source.

In this expression, E_{20} is the UHECR energy in units of 100 EeV, B_{-6} is the magnetic field strength in units of μG, L_{Mpc} is in units of Mpc and $E_c = 1.45 B_{-6} L_{\mathrm{Mpc}}$ (in units of 100 EeV) corresponds to the condition $r_L = L/2\pi$, where $r_L = 0.11 E_{20} B_{-6}^{-1}$ Mpc is the Larmor radius. Note the difference of the above result with the formula given in Ref. [16], for which $D(E) \propto E^{1/3}$ for $E_{20} < E_c$, and $D(E) \propto E$ for $E_{20} > E_c$. The dependence of $D(E)$ for $0.1 E_c < E < E_c$ in Eq. (3) above agrees very well with the phenomenological Bohm diffusion coefficient $D_B \simeq r_L c$.

The diffusive regime as well as the transition to nearly rectilinear propagation can also be seen in the dependence of time delay τ (defined as the difference between the total propagation time and the straight flight distance d/c) on energy E shown in Fig. 6 for $B_{-6} = 1$ and Cen-A as the source: In the diffusive regime the average time delay $\tau(E) \simeq d^2/4D(E)$, where d is the source distance, whereas for $E_{20} \gtrsim 3$, in the regime of almost rectilinear propagation, $\tau(E) \simeq 1.7 \times 10^8$ yr $E_{20}^{-2} d_{\mathrm{CenA}}^2 L_{\mathrm{Mpc}} B_{-6}^2$ [11], where $d_{\mathrm{CenA}} \equiv d/3.4$ Mpc. The values obtained for $D(E) \simeq d^2/4\tau(E)$ from Fig. 6 in the diffusive regime are consistent with Eq. (3) within the width of the distribution.

Note that according to Eq. (3) a largest eddy size L_{Mpc} considerably smaller than 1 would lead to less diffusion, tending to make anisotropies even larger. We remark that indeed L_{Mpc} is likely to be smaller [23] and thus the choice $L_{\mathrm{Mpc}} = 1$ Mpc is already a conservative choice in favor of the single-source model.

Using these results, one can understand the situation encountered in the previous section. In the diffusive regime one finds that the ratio of the diffusive propagation time (which is equal to the time delay in this approximation) to the source distance reads $\tau(E)/d \simeq 13 E_{20}^{-2} B_{-6}^2 L_{\mathrm{Mpc}} d_{\mathrm{CenA}}$, for $E_{20} > E_c$. Diffusion ceases to be a good approximation when $\tau(E)/d$ is no longer $\gg 1$. For instance, the conservative choice $\tau(E)/d > 1$ requires $E_{20} < 3 B_{-6} L_{\mathrm{Mpc}}^{1/2}$. This corresponds to a maximal energy for diffusion of $\simeq 100$ EeV when $B \simeq 0.3$ μG, and $\simeq 300$ EeV when $B \simeq 1$ μG. These numbers are in agreement with the results of the previous section. Note that the ratio of the diffusive propagation time to the source distance also corresponds to the ratio of the

source distance to the mean free path for scattering on the magnetic inhomogeneities $\simeq D/c$ to within a factor four.

The difference betwen our results and Ref. [20] can be explained as a misuse of the diffusion coefficient given in Ref. [16] by the authors of Ref. [20], and to some extent, by the fact that that diffusion coefficient itself has the wrong scaling with E, B, and L. More precisely in Ref. [20] the authors use the diffusion coefficient $D(E) \simeq 0.05\ \mathrm{Mpc}^2/\mathrm{Myr}\, E_{20}^{1/3} B_{-6}^{-1/3} L_{\mathrm{Mpc}}{}^{2/3}$ [16] [note that the present prefactor is the correct one; their Eq. (1) has a numerical error] on the whole energy range, whereas according to Ref. [16], this scaling is only valid when $r_L \lesssim L/2\pi$, or as above $E_{20} \lesssim E_c = 1.45 B_{-6} L_{\mathrm{Mpc}}$. This makes an important difference, because, had the authors of Ref. [20] used the other limiting regime they quote, namely $D \simeq 0.1 E_{20} B_{-6}^{-1}\ \mathrm{Mpc}^2/\mathrm{Myr}$, valid for $E_{20} \gtrsim 1.45 B_{-6} L_{\mathrm{Mpc}}$, they would have found that the ratio of the diffusive distance traveled to source distance reads $d/4D \simeq 2.6 E_{20}^{-1} B_{-6} d_{\mathrm{CenA}}$, which shows that $B > 1\ \mu$G is necessary to achieve diffusion up to the highest energies $E_{20} \simeq 3$. Instead, they used the former approximation, giving $d/4D \simeq 5.3 E_{20}^{-1/3} B_{-6}^{1/3} L_{\mathrm{Mpc}}{}^{-2/3} d_{\mathrm{CenA}}$, which due to the (incorrect) weak scaling would let believe that diffusion can be achieved easily with $B \simeq 0.3\ \mu$G on the whole range of energies.

One should mention that the transition between diffusive and rectilinear regimes of propagation is not sudden; it stretches over half an order to an order of magnitude. As one approaches this transition, the anisotropy increases steeply to match the small angle deflection in the rectilinear regime $\theta_E \simeq 140° E_{20}^{-1} B_{-6} L_{\mathrm{Mpc}}{}^{1/2} d_{\mathrm{CenA}}^{1/2}$ [11]. Therefore it is incorrect to assume that the diffusive estimate for the anisotropy remains valid up to the transition energy.

Finally, Ref. [20] (unlike Ref. [29]) also base their calculations for the flux of particles detected at Earth on a time-dependent solution of the diffusion equation, but one should rather use a stationary solution corresponding to a continuously emitting source. Indeed if Cen-A were a bursting source, or more generally a source emitting only once on a timescale $t_{\mathrm{em}} \ll \tau_{\mathrm{min}}$, where τ_{min} is the smallest time delay imparted to all UHECRs, or equivalently, the time delay at the highest energies observed, an experiment like AGASA would record events only in a limited range of energies [33]. In other words the distance d_D of the diffusion front from the source at time t is given by $d_D(E) = 6D(E)t$, and depends on energy. At the present time at which AGASA is operating, the front of low energy particles would not have yet reached the Earth, while that of higher energy particles would already have passed. From Fig. 6 one sees that at any given time AGASA would record only part of the total energy spectrum, since particles with $E = 10$ EeV arrive at time $\tau \sim 10^9$ yr, while particles with $E = 100$ EeV arrive at times $\tau \sim 10^8$ yr.

This implies that if Cen-A is the source of all UHECRs, it has to be a continuously emitting source, or, what amounts to the same, an intermittent source that emits on timescales t_{em}, with quiescent periods of duration $\Delta t \ll \min[\Delta\tau(E)]$. Here $\Delta\tau(E)$ denotes the spread of time delays at energy E, and the condition ensures that the various contributions of the various bursts of particles largely overlap so as to produce a featureless energy spectrum at all times. Furthermore, since no low energy cutoff in the energy spectrum has been seen down to energies $\simeq 5$ EeV, Cen-A must have been active for a time corresponding to the largest time delay possible $\simeq \tau(5\ \mathrm{EeV}) + \Delta\tau(5\ \mathrm{EeV})$. For $B \simeq 1\ \mu$G, we find that Cen-A must have been producing UHECRs intermittently for the past $\simeq 10$ Gyr. Whether this is realistic or not can hardly be constrained on theoretical grounds. The above constraints on the duration of the periods of activity and quiescence t_{em} and Δt read $t_{\mathrm{em}} \lesssim 10^7$ yr, and similarly for Δt, which are reasonable orders of magnitude for the evolution time scale of Cen-A [34]. The age of Centaurus A can be estimated from the time necessary for its jets to extend to their present size $\simeq 250$ kpc, i.e. between $\sim 10^8$ yr and a few Gyr, depending on the deceleration during extension, so that for our purposes this age is essentially unknown. Note that Centaurus A is a radio-galaxy with sub-relativistic jets, and without hot spots; the lobes are not particularly active, with a total bolometric luminosity $\sim 10^{39}$ ergs/s [34].

The constraints of Ref. [20] on the energy requirement must thus be reconsidered. In the stationary regime, the flux at Earth reads $E^2 j(E) = E^2 q(E)/(4\pi)^2 D(E) d$, where $q(E)$ is the injection spectrum at the source. One easily calculates that, assuming $q(E) \propto E^{-2}$, in order to produce the energy weighted flux measured by cosmic ray experiments $\simeq 10^{24.5}\ \mathrm{eV^2 m^{-2} s^{-1} sr^{-1}}$, one requires a UHECR emission power $\mathcal{P}_{\mathrm{UHECR}} \simeq 10^{39} B_{-6}^{-1} d_{\mathrm{CenA}}$ ergs/s at the source. Note that this represents the average power; the actual power during the phase of activity is higher and reads $\mathcal{P}_{\mathrm{UHECR}}(t_{\mathrm{em}} + \Delta T)/t_{\mathrm{em}}$. The above $\mathcal{P}_{\mathrm{UHECR}}$ is thus a strict lower limit, which is nevertheless more optimistic than the $\sim 10^{43}$ ergs/s obtained in Ref. [20].

As an aside, we note that the above constraint on the age of Centaurus A can be generalized to any such source of UHECRs, namely that the time delay at the lowest energies be smaller than the age of the source, and thus also the age of the Universe. The propagation time at 5 EeV reads, using Eq. (3): $\tau \simeq 2.8\ \mathrm{Gyr}\, B_{-6} d_{\mathrm{CenA}}^2$. Imposing $\tau \lesssim 14$ Gyr gives a general constraint between the distance d to the source and the strength of the intervening magnetic field:

$$\left(\frac{B}{1\ \mu\mathrm{G}}\right)\left(\frac{d}{10\ \mathrm{Mpc}}\right)^2 \lesssim 0.6. \tag{4}$$

Even if there are several sources contributing to the cosmic ray flux, this limit should hold unless the sources conspire to add their individual piecewise contribution in such a way as to form a featureless energy spectrum. When there are many sources the above constraint disappears, as the central limit theorem would guarantee that a featureless spectrum would be produced; this is notably one of the peculiarities of the γ-ray burst model of UHECR origin [35].

IV. CONCLUSIONS

Our detailed numerical simulations show that the model considered in Ref. [20], in which Centaurus A is the source of all observed UHECRs, is inconsistent with the data, at

least for the magnetic field strength $B \simeq 0.3$ μG put forward by these authors. We find that for a magnetic field strength $B \simeq 1$ μG, the predicted energy spectrum is in marginal agreement with that observed by AGASA. However the large deflection angle of the highest energy event (the Fly's Eye event) with respect to the line of sight to Cen-A must be explained as a $\simeq 2\sigma$ fluctuation. We also argued that this magnetic field intensity saturates the observational upper bounds from Faraday rotations and on x-ray emission from the ambient gas. This model can be tested by improving these upper limits with current experiments. We also showed that in order to explain all UHECRs down to $E \simeq 5$ EeV, Cen-A must have been producing UHECRs for the past $\simeq 10$ Gyr. All these facts are rather strong requirements on the source and on the intervening magnetic fields.

However this requirement on the magnetic field intensity could be lowered by an order of magnitude if the UHECR primaries are iron nuclei instead of protons. Heavy nuclei are further deflected by significant amounts after traversal of the galactic magnetic field, which would improve the isotropy on large angular scales. However photodisintegration of heavy nuclei on the cosmic microwave background (CMB) is sufficiently severe that no UHECR of energy greater than 200 EeV could have traveled longer than 10 Mpc [37]. Here as well, this may be in conflict with the observation of the Fly's Eye event with $E \simeq 3.2 \pm 0.9 \times 10^{20}$ eV observed 136° away from Cen-A; however the disagreement is marginal and deflection in the galactic magnetic field alone could be $\sim 30°$ [21,31], and possibly more, depending on the galactic latitude of incidence and the detailed vertical scale height of the magnetic field. Heavy nuclei primaries thus remain an interesting possibility. A detailed study of their arrival directions distributions and energy spectra is intricate as one needs to follow the mini-shower induced by photodisintegration in the CMB, but is now underway.

Independently of the charge of the primary, it appears more likely that a few sources (instead of a single source) within $\simeq 10$ Mpc from the Earth are responsible for the observed ultrahigh-energy cosmic ray flux, and that the ambient magnetic field strength in the local supercluster $B \sim \mathcal{O}(0.1)$ μG. Work is in progress to quantify the number of sources and their distance scale for various values of the magnetic field strength needed to reproduce the large angular scale isotropy and small angular scale anisotropy as well as the energy spectrum observed by current or past experiments. Ongoing and future ultrahigh-energy cosmic ray experiments [5,6,25], by increasing the statistics at the highest energies, will soon provide much tighter bounds on the number of UHECR sources.

ACKNOWLEDGMENTS

G.S. would like to thank Luis Anchordoqui, Pasquale Blasi, Glennys Farrar, Haim Goldberg, Tsvi Piran, and Tom Weiler for detailed discussions of this subject.

[1] K. Greisen, Phys. Rev. Lett. **16**, 748 (1966); G. T. Zatsepin and V. A. Kuzmin, Pis'ma Zh. Éksp. Teor. Fiz. **4**, 114 (1966) [JETP Lett. **4**, 78 (1966)].

[2] D. J. Bird *et al.*, Phys. Rev. Lett. **71**, 3401 (1993); Astrophys. J. **424**, 491 (1994); **441**, 144 (1995).

[3] See, e.g., M. A. Lawrence, R. J. O. Reid, and A. A. Watson, J. Phys. G **17**, 733 (1991), and references therein; see also http://ast.leeds.ac.uk/haverah/hav-home.html

[4] N. N. Efimov *et al.*, in *Proceedings of the International Symposium on Astrophysical Aspects of the Most Energetic Cosmic Rays*, edited by M. Nagano and F. Takahara (World Scientific, Singapore, 1991), p. 20; B. N. Afnasiev, in *Proceedings of the International Symposium on Extremely High Energy Cosmic Rays: Astrophysics and Future Observatories*, edited by M. Nagano (Institute for Cosmic Ray Research, Tokyo, 1996), p. 32.

[5] D. Kieda *et al.*, Proceedings of the 26th ICRC, Salt Lake, 1999, www.physics.utah.edu/Resrch.html

[6] M. Takeda *et al.*, Astrophys. J. **522**, 225 (1999); M. Takeda *et al.*, Phys. Rev. Lett. **81**, 1163 (1998); N. Hayashida *et al.*, Astrophys. J. **522**, 225 (1999); www-akeno.icrr.u-tokyo.ac.jp/AGASA/

[7] For recent reviews, see J. W. Cronin, Rev. Mod. Phys. **71**, S165 (1999); P. Bhattacharjee and G. Sigl, Phys. Rep. **327**, 109 (2000); A. V. Olinto, *ibid.* **333-334**, 329 (2000); X. Bertou, M. Boratav, and A. Letessier-Selvon, Int. J. Mod. Phys. A **15**, 2181 (2000).

[8] See, e.g., P. L. Biermann, J. Phys. G **23**, 1 (1997).

[9] G. Sigl, D. N. Schramm, and P. Bhattacharjee, Astropart. Phys. **2**, 401 (1994).

[10] J. W. Elbert and P. Sommers, Astrophys. J. **441**, 151 (1995).

[11] E. Waxman and J. Miralda-Escudé, Astrophys. J. Lett. **472**, L89 (1996).

[12] J. P. Vallée, Fundam. Cosmic Phys. **19**, 1 (1997).

[13] D. Ryu, H. Kang, and P. L. Biermann, Astron. Astrophys. **335**, 19 (1998).

[14] P. Blasi, S. Burles, and A. V. Olinto, Astrophys. J. Lett. **514**, L79 (1999).

[15] K. T. Kim *et al.*, Nature (London) **341**, 720 (1989).

[16] P. Blasi and A. V. Olinto, Phys. Rev. D **59**, 023001 (1999).

[17] G. Sigl, M. Lemoine, and P. Biermann, Astropart. Phys. **10**, 141 (1999).

[18] M. Lemoine, G. Sigl, and P. Biermann, astro-ph/9903124.

[19] E.-J. Ahn, G. Medina-Tanco, P. L. Biermann, and T. Stanev, astro-ph/9911123.

[20] G. R. Farrar and T. Piran, astro-ph/0010370.

[21] G. Medina-Tanco, E. M. De Gouveia Dal Pino, and J. E. Horvath, astro-ph/9707041.

[22] L. A. Anchordoqui and H. Goldberg, Phys. Rev. D (to be published), hep-ph/0106217; T. Stanev, Astrophys. J. **479**, 290 (1997).

[23] E. Waxman and J. Bahcall, Phys. Rev. D **59**, 023002 (1998).

[24] G. Medina-Tanco and T. A. Ensslin, Astropart. Phys. **16**, 47 (2001).

[25] J. W. Cronin, Nucl. Phys. B (Proc. Suppl.) **28B**, 213 (1992); The Pierre Auger Observatory Design Report (second edition), 1997; see also http://www.auger.org/ and http://wwwlpnhep.in2p3.fr/auger/welcome.html
[26] P. Sommers, Astropart. Phys. **14**, 271 (2001); N. W. Evans, F. Ferrer, and S. Sarkar, astro-ph/0103085; Y. Ide, S. Nagataki, and S. Tsubaki, astro-ph/0106182; G. A. Medina Tanco and A. A. Watson, Astropart. Phys. **12**, 25 (1999).
[27] D. B. Cline and F. W. Stecker, OWL/AirWatch science white paper, astro-ph/0003459; see also http://lheawww.gsfc.nasa.gov/docs/gamcosray/hecr/OWL/
[28] R. Benson and J. Linsley, Proc. Southwest. Reg. Conf. Astron. Astrophys. **7**, 161 (1981); see also http://www.ifcai.pa.cnr.it/Ifcai/euso.html
[29] L. A. Anchordoqui, H. Goldberg, and T. Weiler, Phys. Rev. Lett. **87**, 081101 (2001).
[30] S. P. Boughn, Astrophys. J. **526**, 14 (1999).
[31] D. Harari, S. Mollerach, and E. Roulet, J. High Energy Phys. **08**, 022 (1999); **02**, 035 (2000); **10**, 047 (2000).
[32] F. Casse, M. Lemoine, and G. Pelletier, Phys. Rev. D **65**, 023002 (2001).
[33] J. Miralda-Escudé and E. Waxman, Astrophys. J. Lett. **462**, L59 (1996).
[34] F. P. Israel, Astron. Astrophys. Rev. **8**, 237 (1998).
[35] E. Waxman, Phys. Scr., T **T85**, 117 (2000), and references therein.
[36] P. G. Tinyakov and I. I. Tkachev, Pisma Zh. Eksp. Teor. Fiz. **74**, 3 (2001) [JETP Lett. **74**, 1 (2001)].
[37] L. N. Epele and E. Roulet, J. High Energy Phys. **10**, 009 (1998); Phys. Rev. Lett. **81**, 3295 (1998).